NASA Technical Paper 1782

Flight Evaluation of a Simplified Gross Thrust Calculation Technique Using an F100 Turbofan Engine in an F-15 Airplane

Frank J. Kurtenbach and Frank W. Burcham, Jr.

JANUARY 1981

NASA

Flight Evaluation of a Simplified Gross Thrust Calculation Technique Using an F100 Turbofan Engine in an F-15 Airplane

Frank J. Kurtenbach and Frank W. Burcham, Jr.
Dryden Flight Research Center
Edwards, California

FLIGHT EVALUATION OF A SIMPLIFIED GROSS THRUST CALCULATION

TECHNIQUE USING AN F100 TURBOFAN ENGINE IN AN

F-15 AIRPLANE

Frank J. Kurtenbach and Frank W. Burcham, Jr.
Dryden Flight Research Center

INTRODUCTION

The in-flight determination of jet engine gross thrust has been, and will continue to be, of major importance in the flight test environment, since it is directly related to the ability to determine aircraft performance. As the complexity of jet engines has increased, the instrumentation, computation, and engine testing necessary to determine thrust has also increased. At present we are able to determine the gross thrust of modern engines to an acceptable degree of accuracy only by using a very complex gas generator method (GGM), which requires extensive instrumentation and engine testing (refs. 1 to 3). As an alternative, a simplified gross thrust model (SGTM) method has been developed (ref. 4). The SGTM is based on the measurement of three pressures in the afterburner, and it has already been applied to turbojet engines (refs. 5 and 6).

As part of a flight program to study propulsion system integration on the F-15 airplane, the NASA Dryden Flight Research Center conducted an evaluation of the SGTM on the F100 afterburning turbofan engine. The two F100 engines to be made available for the flight evaluation had undergone calibration tests in the NASA Lewis Research Center Propulsion System Laboratory. During these calibration tests, the coefficients for the SGTM were developed, engine airflow was determined, and the GGM and SGTM results were compared with measured thrust. Reference 3 provides a comparison of the measured thrust to the results of the engine manufacturer's GGM. It also develops a set of corrections to make the GGM agree with the measured thrust of the test engines. This "calibrated" GGM is discussed in reference 7, and was used to derive the results presented herein.

This paper reports an evaluation of the SGTM using flight data. The left engine of the F-15 was instrumented for both the GGM and the SGTM input measurements. The evaluation was conducted at Mach numbers from 0.6 to 1.5, at altitudes from 6000 meters to 13,700 meters, and at power settings from idle to maximum afterburning.

1

SYMBOLS AND ABBREVIATIONS

A	area, m^2
BOM	bill of material
C_D	nozzle discharge coefficient
C_V	nozzle velocity coefficient
C_Y	SGTM empirical coefficient
E	SGTM empirical coefficient
F_G	gross thrust, kN
FIGV	fan inlet guide vane angle, deg
GGM	gas generator method
K_1	SGTM empirical coefficient
K_2	SGTM empirical coefficient
M	Mach number
N_{fan}	fan rotation speed, rpm
PR	pressure ratio
p	static pressure, N/cm^2
p_t	total pressure, N/cm^2
SGTM	simplified gross thrust model
T_t	total temperature, K
W	mass flow, kg/sec
W_{fp}	primary (gas generator) fuel flow, kg/hr
W_{ft}	total (primary plus afterburner) fuel flow, kg/hr

γ ratio of specific heats

θ $T_{t_2}/288.7$

Subscripts:

a   absolute pressure measurement

d   differential pressure measurement

geom   geometric

j   jet (nozzle throat)

ref   reference

Superscript:

$'$ functionally correlatable value

Engine stations (fig. 3):

0   free stream

2   engine fan inlet

6   low pressure fan-turbine exit

6.5   augmentor liner, flameholder

6.7   augmentor liner

6.9   augmentor liner at entrance to nozzle

7   nozzle throat

8   nozzle exit

AIRPLANE DESCRIPTION

The F-15 airplane (fig. 1) is a high performance fighter with a Mach number capability of 2.5. It is powered by two F100 afterburning turbofan engines located in the aft fuselage.
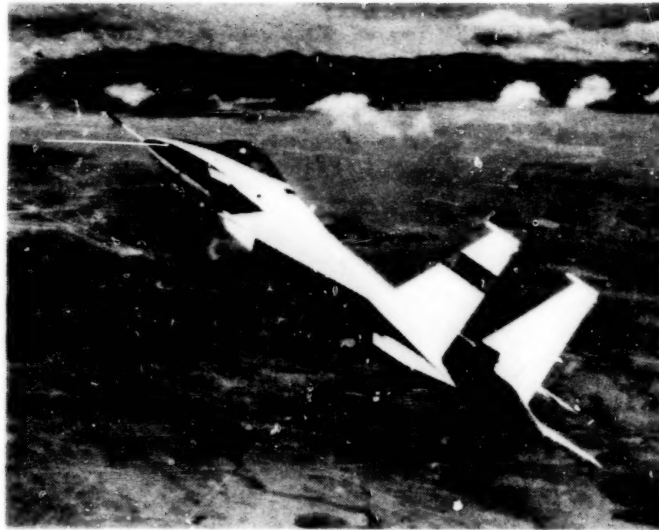
Figure 1.   F-15 test aircraft.

ENGINE DESCRIPTION

The F100-PW-100 engine (fig. 2) is a low bypass twin spool afterburning turbo-fan. The three-stage fan is driven by a two-stage low pressure turbine. The 10-stage high pressure compressor is driven by a 2-stage high pressure turbine. The engine incorporates variable fan inlet guide vanes and rear compressor variable vanes to achieve high performance over a wide range of power settings. Continuously variable thrust augmentation is provided by a mixed flow afterburner, which exhausts through a variable area convergent-divergent nozzle. The engines involved in the SGTM evaluation carried serial numbers P680059 and P680063 (hereafter referred to as 059 and 063). Each engine was designated a prototype 2 7/8 engine, and consisted of a series 2 core (compressor, combustor, high pressure turbine, and exhaust nozzle) and a series 3 fan and low pressure turbine. The control logic and schedules were intermediate to the series 2 and 3 engines. Therefore, the results are not totally representative of production F100 engines. More information on the test engines is given in reference 7.
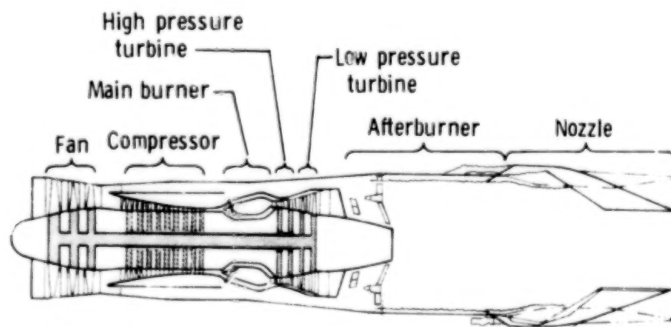

Figure 2.   Schematic representation of F100-PW-100 engine.

4

Both engines were tested in the altitude facility (refs. 7 to 9). Only engine 059 was tested in flight, installed in the left side of an F-15 airplane.

DATA ACQUISITION SYSTEM

The data acquisition system on the F-15 airplane measured and recorded over 350 parameters for the propulsion-airframe integration program. Only the parameters of interest for the evaluation of the SGTM are discussed here.

Engine Instrumentation

The instrumentation installed in engine 059 is shown in figure 3. All instrumentation was for steady state data only.

(a) Station locations.
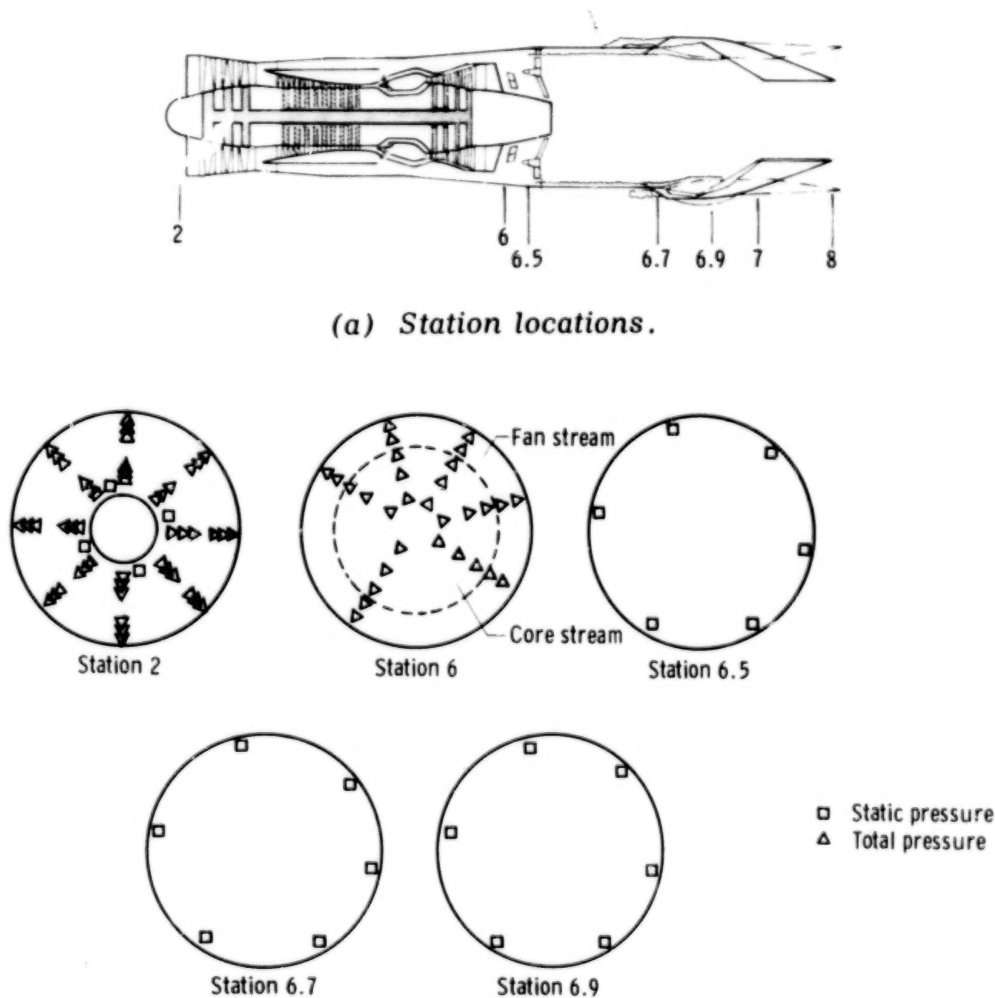
(b) Individual stations.

Figure 3. Engine instrumentation.

Station 2 pressures.—The station 2 compressor face rake array consisted of eight equally spaced rakes: each had six total pressure probes located at the centers of equal areas. To increase measurement accuracy, differential pressure transducers were used to measure the total pressures at this station. A static pressure port in the inlet was used as the source of the reference pressure for the differential transducers. A tank was installed in the reference system to eliminate any pressure lag effects, and a special high accuracy digital quartz transducer was used to measure the reference pressure. All the transducers at station 2 were in a temperature-controlled environment.

Station 6 pressures.—The station 6 instrumentation consisted of an array of 30 total pressure probes on six rakes: 12 in the fan duct stream and 18 in the core stream. Also included was a bill of material (BOM) total pressure probe, an averaging probe with ports in the fan and core streams all open to a common plenum and measured by a single transducer. The BOM probe was designed to be used only for ground engine trimming.

Afterburner static pressures.—Station 6.5, 6.7, and 6.9 instrumentation consisted of six static pressure ports located at approximately equal circumferential positions on the afterburner liner. It would have been desirable to measure the station 6, 6.5, and 6.9 pressures with differential transducers, as was done at station 2. However, only a few differential transducers were available, so most of the station 6 pressures were measured with less accurate absolute transducers, which for this application could not be located in a temperature-controlled environment.

In reference 6, it is pointed out that the SGTM is very sensitive to the difference between p_{t_6} and $p_{6.9}$. Therefore, a more accurate system using differential pressure transducers and the reference pressure system shown in figure 4 was used to measure the pressures. Differential pressure transducers were used for the $p_{6.5}$ and $p_{6.9}$
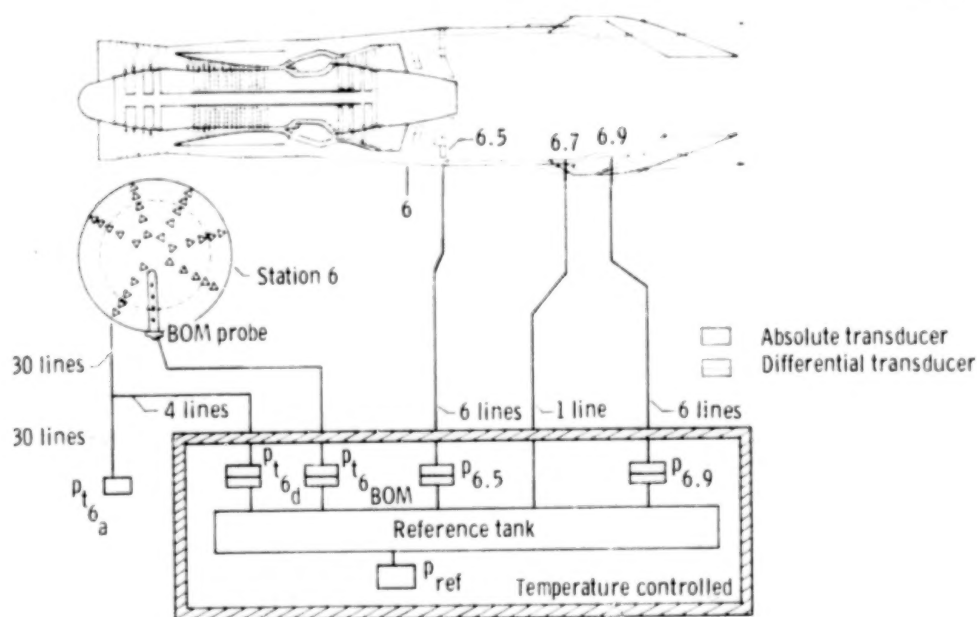

Figure 4. Schematic of pressure measurement system for stations 6, 6.5, and 6.9.

static pressures, the BOM p_{t_6} probe, and four of the 30 p_{t_6} probes. These transducers were located in a temperature-controlled environment. The reference pressure source was obtained from a port at station 6.7 and was measured with a single absolute transducer located in a temperature-controlled environment. In addition to the four p_{t_6} probes measured with differential transducers, all 30 p_{t_6} probes were measured with absolute transducers.

Other engine parameters.—Nozzle area was determined by use of a special engine-mounted linear potentiometer that was connected to the nozzle components downstream of the actuating cables.

Primary (gas generator) fuel flow and engine total fuel flow were measured by using volumetric flowmeters that were laboratory calibrated. Fuel temperature measurements at each flowmeter location provided specific gravity values for converting the volumetric reading to mass flows.

The fan inlet guide vane angle (FIGV), which is necessary for the determination of total engine airflow, was measured by engine-mounted linear potentiometers.

The engine fan speed was obtained from a speed sensor mounted at the bottom of the engine case.

Other airplane parameters.—Airplane total and static pressure were sensed on a nose boom pitot-static system. Static pressure position error was corrected in the air data computer. Total temperature was measured, along with numerous other parameters.

Recording System

The signals from the various airplane and engine sensors were signal conditioned and digitized by a pulse code modulation (PCM) system with eight-bit resolution. In cases where greater resolution was required, the incoming signal was divided into high and low levels and recorded on two eight-bit words. The outputs of the digital transducers were handled in this way, as was the reference pressure for the system shown in figure 4. The digital information was recorded on board by a tape recorder and was also telemetered to the ground for recording and real time display.

The pressure and position transducers were calibrated on board the aircraft with the complete data system operating. In addition, all pressure measurements were compared to ambient pressure under static conditions before and after each flight. These data provided information on transducer calibration zero shifts. If the pre- and postflight zero shifts were consistent, the transducer calibration was zero shifted accordingly. If inconsistent, the transducer reading was eliminated from the data set. No attempts were made to progressively zero shift the transducer calibration during the flight.

Pressure line lengths for some measurements exceeded 6 meters. However, the test conditions were established in steady state flight. so no lag corrections were necessary.

PARAMETER UNCERTAINTIES

The parameters involved in the calculation of the SGTM and the GGM are shown in table 1 along with the parameter range and the probable uncertainty.

The probable uncertainty is due to the sensor uncertainty and, more importantly, to the resolution error of the eight-bit PCM system.

TABLE 1.—PARAMETER UNCERTAINTY

Parameter	Range	Uncertainty	Applicable to.	
			SGTM	GGM
P_0. N/cm^2	0 to 10.2*	±0.031	X	X
$P_{2_{ref}}$. N/cm^2	0 to 34*	±0.014	---	X
P_{t_2}. N/cm^2	±4	±0.031	---	X
$P_{t_{6_a}}$. N/m^2	0 to 34	±0.175	X	X
P_{ref}. N/cm^2	0 to 34*	±0.092	X	---
$P_{t_{6_d}}$. $P_{t_{6_{BOM}}}$. N/cm^2	±4	±0.031	X	X
$P_{6.5}$. N/cm^2	±4	±0.031	X	---
$P_{6.9}$. N/cm^2	±4	±0.031	X	---
T_{t_2} (T_{t_0}). K	222 to 533	±1.9	---	X
FIGV. deg	-25 to -5	±0.53	---	X
N_{fan}. rpm	500 to 12,000*	±12	---	X
A_j. cm^2	0.251 to 0.604	±0.0046	---	X
W_{fp}. kg/hr	326 to 26.943*	±22.7	---	X
W_{ft}. kg/hr	2395 to 59.874*	@6800 ± 73	---	X

*Recorded on two 8-bit PCM channels.

The values in table 1 reflect only the uncertainty in the measurement; they do not reflect the effects of probe design or inadequate probe coverage.

TEST CONDITIONS AND PROCEDURES

The flight conditions at which data were acquired are shown in figure 5. Also shown are the altitude facility test conditions at which the test engines were calibrated. The flags on the symbols indicate power setting on the test engine. As the figure shows, no power settings below intermediate were tested at supersonic speeds, and only one test was performed at maximum power. The test points at high altitudes (above 10,000 meters) and subsonic Mach numbers were of special interest because of the low pressure levels and low thrust values involved, and are discussed later. The usual test procedure was to stabilize the airplane at the desired flight conditions with the desired power setting on the left engine. Ten to 20 seconds of stabilized data were taken. Computations were performed at one per second, and 5 seconds of results were averaged.
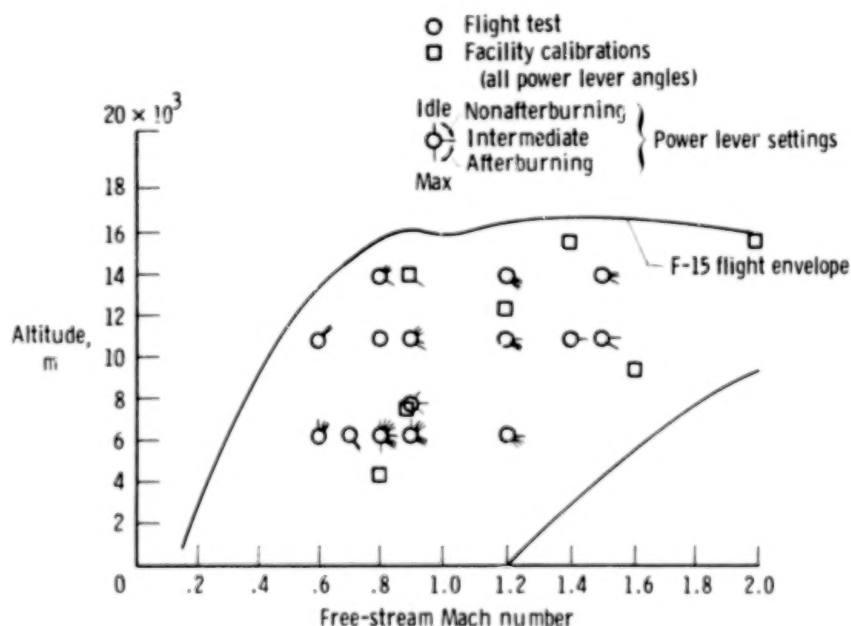

Figure 5. Flight test and facility calibration conditions.

The value of p_{t_6} was of key importance to the SGTM, and of less importance to the GGM. The average of the 30 p_{t_6} probes as determined from the absolute transducers did not correlate well with the average of the four differential transducers. This is believed to be due to the much poorer accuracy of the absolute transducers, which had

9

a measurement range four times as large as that of the differential transducers, and the lack of a temperature-controlled environment. Therefore, a method was developed to use the four differential p_{t_6} measurements to correct the average of the 30 p_{t_6} absolute transducer readings. This correction was large only for the high altitude subsonic data, but it was applied to data acquired at all flight conditions.

ENGINE THRUST MODELS

Gas Generator Performance Model

The manufacturer's engine model (ref. 10 and fig. 6) is a gas generator analysis model which relies primarily on the measurement of total pressu.e and nozzle area for the determination of gross thrust. The model uses a combination of theoretical values, component test data, and full-scale engine data to generate the relationships necessary for the analysis.
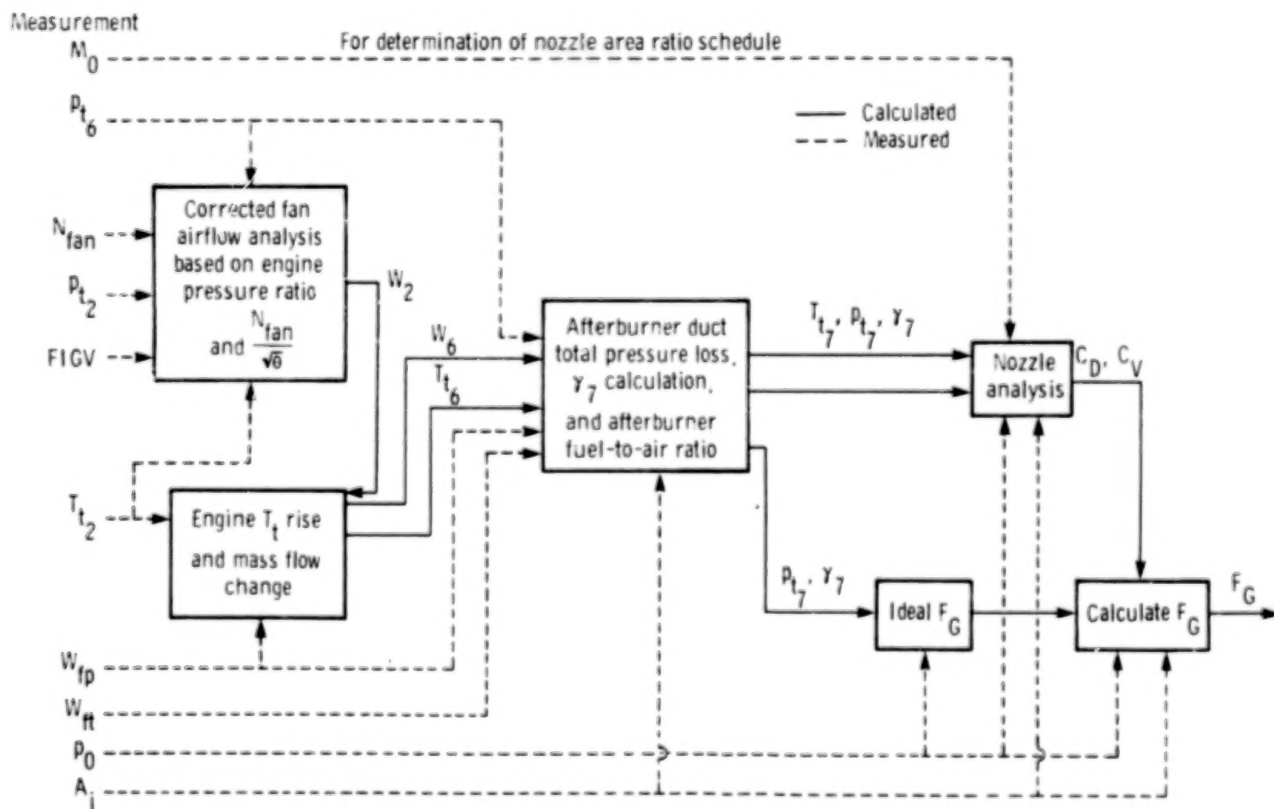

Figure 6. Engine gas generator performance model.

First, corrected fan airflow is computed as a function of engine pressure ratio and corrected fan speed. Then station 6 total temperature, T_{t_6}, is computed as a function of engine core fuel-to-air ratio and inlet temperature. An analysis of the

afterburner flow characteristics provides nozzle inlet total temperature, T_{t_7}; total pressure. p_{t_7}; and the ratio of specific heats, γ_7. The latter two parameters are combined with free-stream ambient pressure to determine an ideal gross thrust. Nozzle discharge and velocity coefficients are determined from p_{t_7}; nozzle area ratio, A_j; and γ_7. Station 6 total temperature, T_{t_6}, is used to determine nozzle thermal expansion. The ideal thrust is combined with the nozzle coefficients to compute the actual gross thrust.

References 1 and 2 discuss the application of a gas generator method of this type on a similar engine and indicates the effect of measurement uncertainties on the thrust computation.

Simplified Gross Thrust Model

The simplified gross thrust model as developed in reference 4 is based on a one-dimensional analysis of the flow in the augmentor and nozzle. Calibration factors are required to account for three-dimensional effects, the effects of friction and mass transfer, and the effects of the simplifying assumptions used in the theory. The model is shown schematically in figure 7.
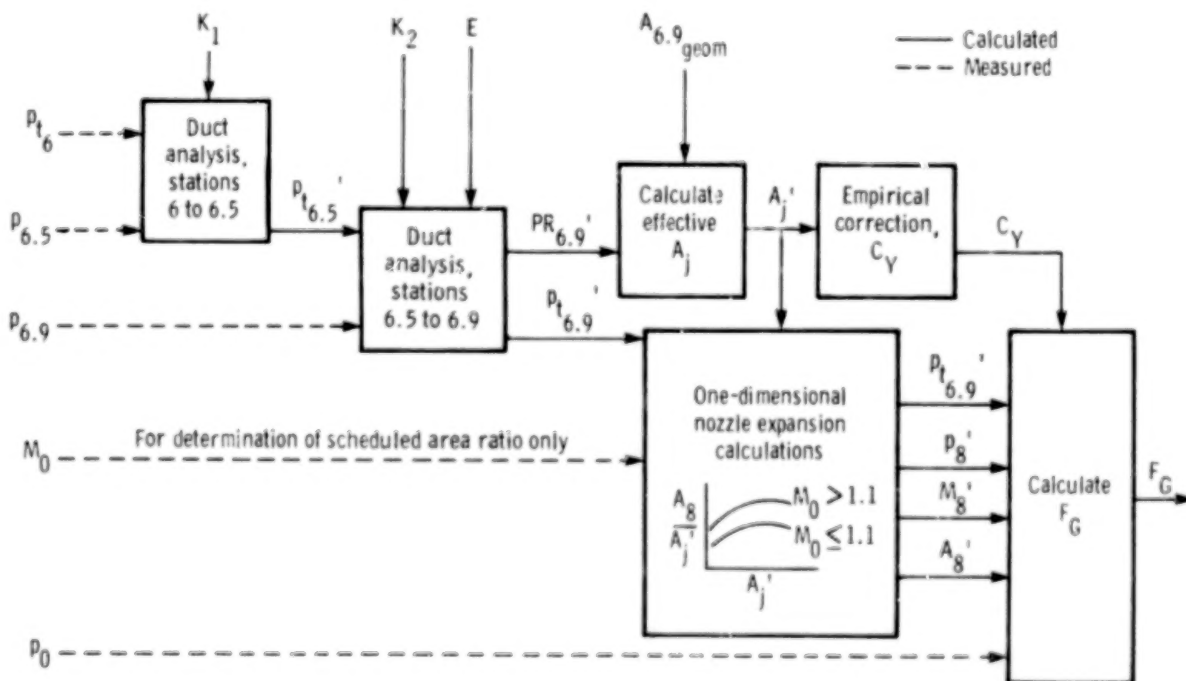

Figure 7. Simplified gross thrust model. Choked flow case, $\gamma = 1.3$.

Four coefficients are used in the technique: K_1, K_2, E, and C_Y. Both K_1 and K_2 are constant; E and C_Y vary with engine operating condition as follows.

$$E = f\left(p_{t_6}, \ p_{6.5}, \ p_0\right)$$

$$C_Y = f\left(A_j\right)$$

The coefficients were determined from the altitude test data in reference 7 by an iterative technique which seeks to minimize thrust error.

The theoretical basis of the technique is discussed in reference 4. This model analyzes the afterburner duct as a one-dimensional continuous flow using influence coefficient relationships, where the functional relationships are dealt with in differential form. Influence coefficients are discussed in reference 11 (pp. 226 to 232). For clarity, parameters calculated by the SGTM are identified by a prime (') to indicate that they are based on an empirically corrected one-dimensional analysis. These values can be considered to be functionally correlatable in that they provide repeatable values of gross thrust. This is not to imply that the values necessarily differ greatly from true values.

The measurements necessary for the SGTM are turbine discharge total pressure, p_{t_6}; flameholder static pressure, $p_{6.5}$; nozzle inlet static pressure, $p_{3.9}$; and free-stream static pressure, p_0. As stated previously, the nozzle divergent area ratio is scheduled as a function of nozzle throat area, A_j, and free-stream Mach number, M_0, so M_0 must also be input. The technique also requires the cold geometric area at station 6.9, $A_{6.9_{geom}}$.

The simplified gross thrust model then uses the calculation of nozzle throat total pressure, $p_{t_{6.9}}'$, and effective area, A_8', for the calculation of gross thrust. More details of the calculation procedure are given in reference 6.

RESULTS AND DISCUSSION

Thrust Model Uncertainty

Simplified gross thrust model.--Uncertainties in the calculated values for the SGTM were computed by using the following technique. First, the gross thrust was calculated by using the measurements as recorded. Second, each of the input measurements was changed by a percentage of the full-scale value of the transducer, and the percentage of change in gross thrust was calculated. Typical results are shown in figure 8 for four power settings at Mach 0.8 and an altitude of 4020 meters.
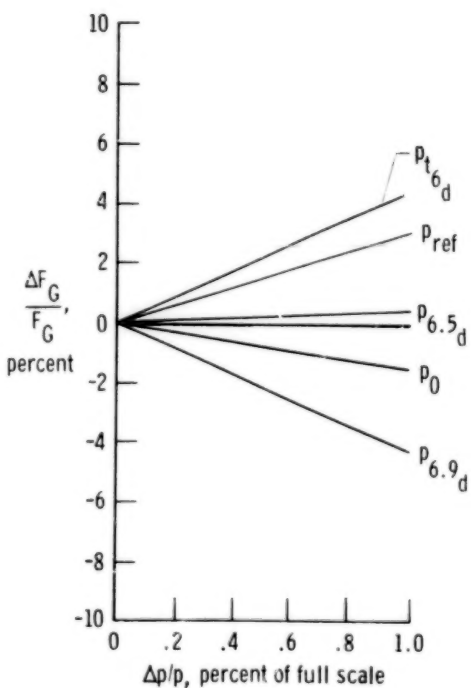
It is apparent that p_{t_6} and $p_{6.9}$ have the greatest impact on gross thrust. Reference pressure and ambient pressure are also important, and $p_{6.5}$ has a small effect. For a given percentage of error in the pressure measurements, the change
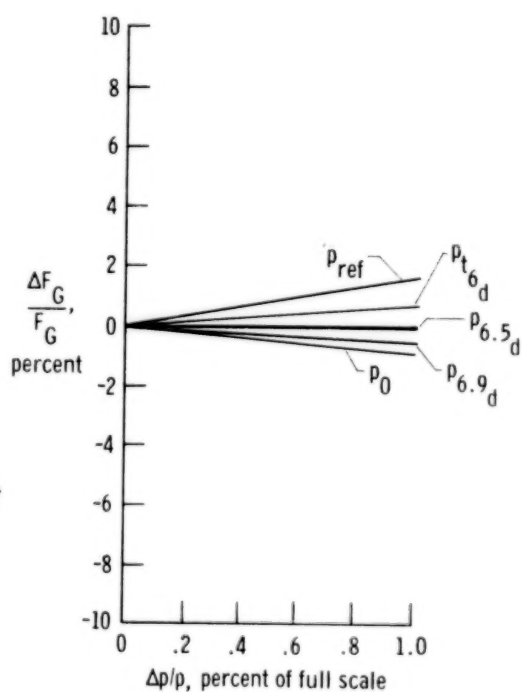
12
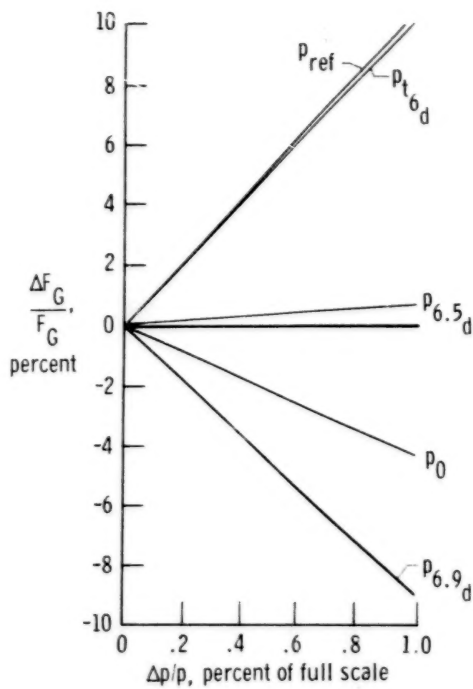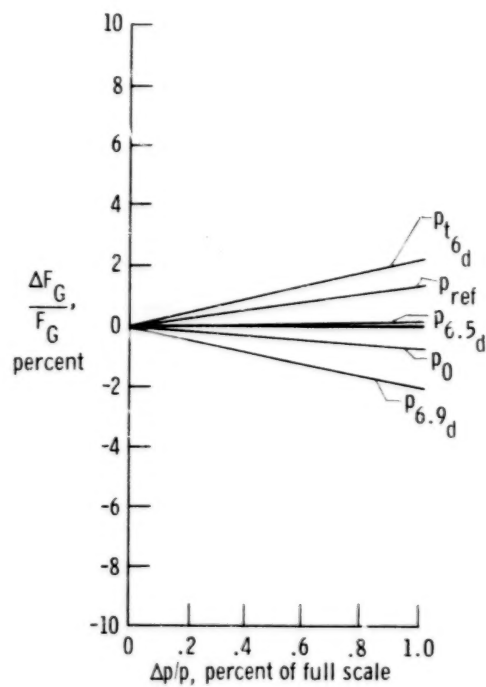
(a) Idle power.

(c) Intermediate power.

(b) Part power.

(d) Maximum power.

Figure 8. Effect of changes of measured pressures on gross thrust computed with SGTM.

in gross thrust is greatest at idle power and decreases as power setting increases. For example, a 1 percent change in $p_{6.9_d}$ while at idle power causes a -9 percent change in gross thrust, while at maximum power the 1 percent change in $p_{6.9_d}$ causes only a -0.8 percent change in thrust.

Calculations like those shown in figure 8 were made at several conditions in the flight envelope. The results were then multiplied by the probable uncertainti s of the measurements (table 1) to provide an estimate of the uncertainty in gross thrust due to each measurement. The uncertainties of each measurement were then combined by using a root-sum-square technique to obtain the overall gross thrust uncertainty. It was found that over the flight envelope and power setting range these uncertainty values were primarily a function of $p_{t_6} - p_{6.9}$. This relationship is shown in figure 9.
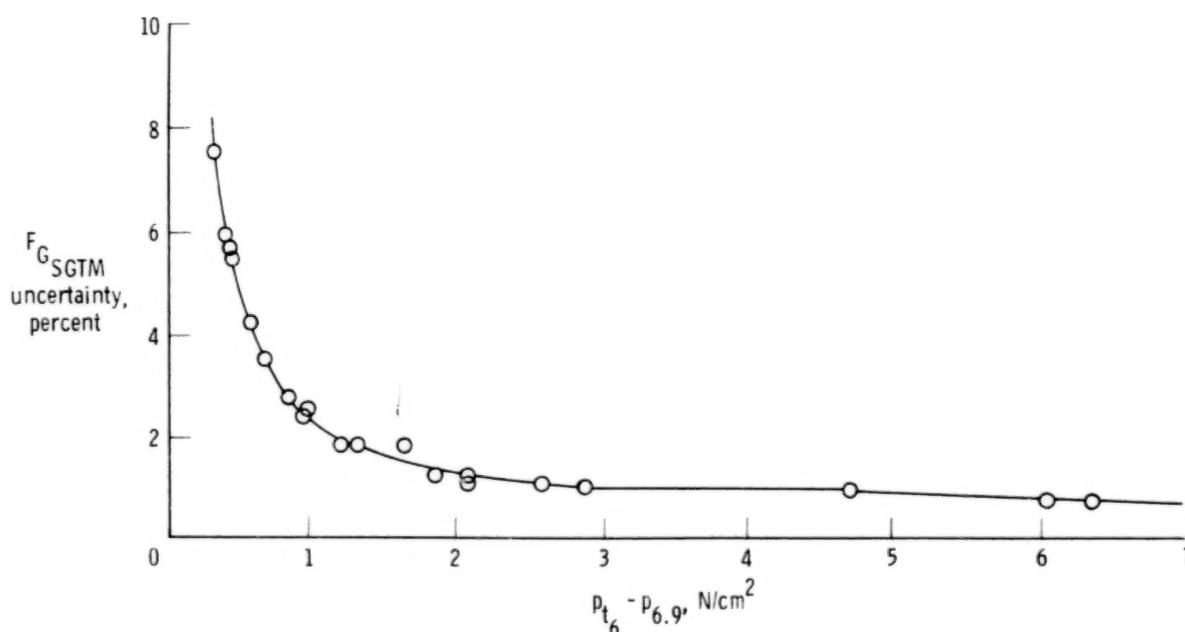

Figure 9. Uncertainty in SGTM.

For values of $p_{t_6} - p_{6.9}$ greater than 2 N/cm^2, the estimated uncertainty is ±1 percent. At lower values of $p_{t_6} - p_{6.9}$, uncertainty increases rapidly. This corresponds to either low power settings or flight at high altitudes and low speeds, both of which cause low density flow in the afterburner.

Gas generator model.—The uncertainty of the GGM gross thrust was computed in a manner similar to that used for the SGTM. The uncertainty of the GGM was determined for altitude facility test conditions and is reported in reference 3. These results were recomputed to derive the uncertainties due to the pressure transducers used in the flight evaluation. The data collapsed, as shown in figure 10, for all flight conditions when plotted versus $p_{t_6} - p_{6.9}$. The trend of the data is similar
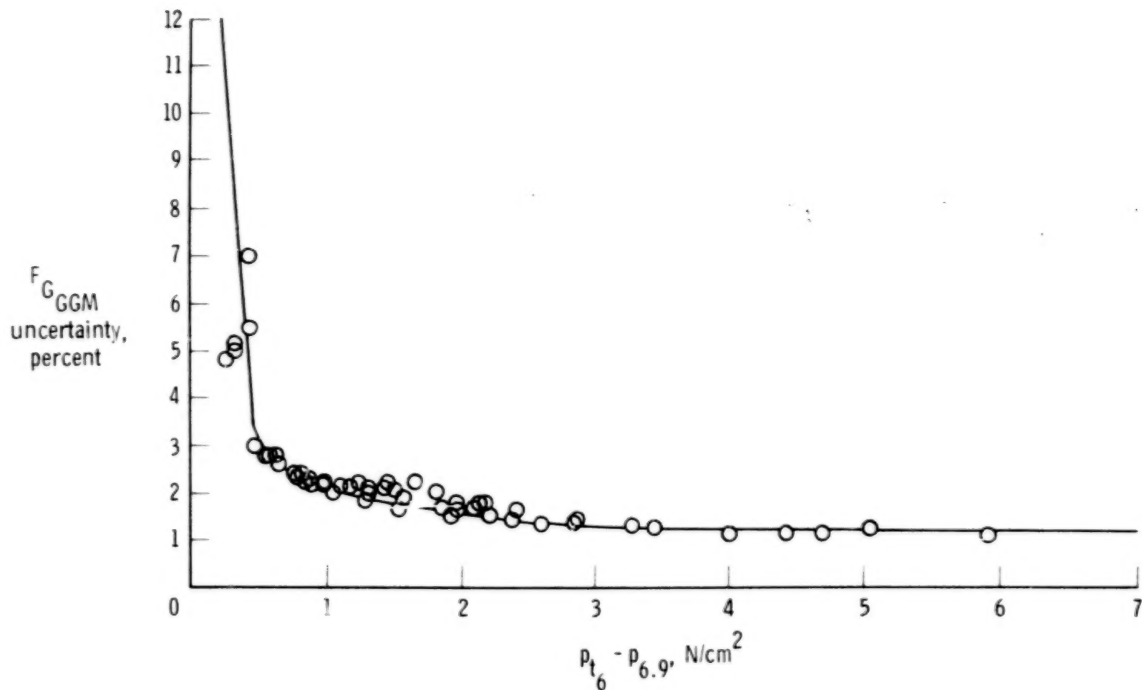
14

Figure 10. Uncertainty in gas generator model.

to that for the uncertainties for the SGTM. For values of $p_{t_6} - p_{6.9}$ of 3 N/cm^2 and above, the GGM uncertainty is ±1 percent, while for lower values of $p_{t_6} - p_{6.9}$, uncertainty increases.

Combined model uncertainty.—Since the GGM will be used to evaluate the SGTM, the uncertainty of the evaluation will depend on the combined uncertainty of the GGM and the SGTM. The results of figures 9 and 10 were combined using a root-sum-square method, and the resulting uncertainty of evaluation is shown in figure 11.
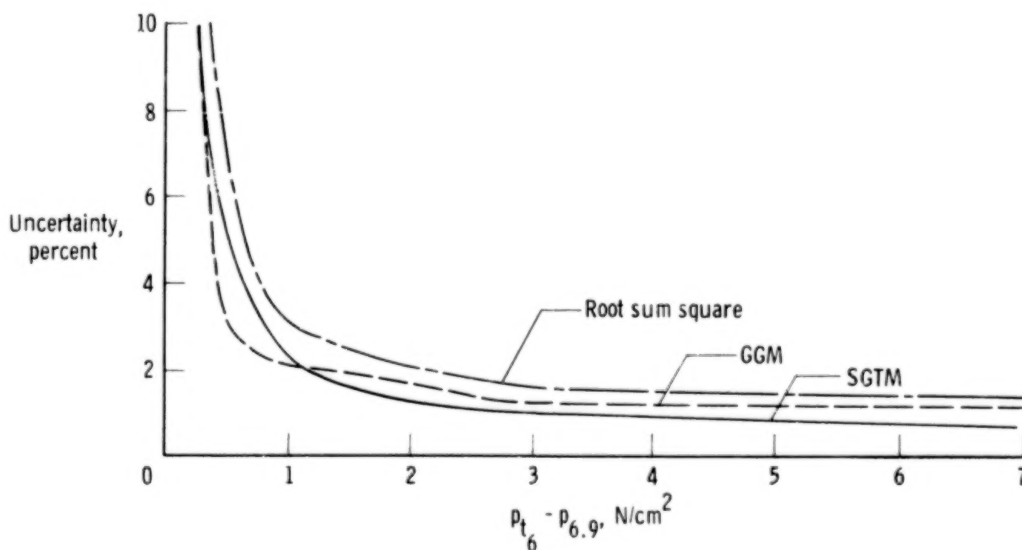

Figure 11. Expected uncertainty of the combined GGM and SGTM.

15

The uncertainty ranges from 10 percent at low values of $p_{t_6} - p_{6.9}$ to 1.4 percent for high values of $p_{t_6} - p_{6.9}$. For all values of $p_{t_6} - p_{6.9}$ of 2 or above, the expected uncertainty is within 2 percent.

Comparison of Methods

The difference between the calculated values of the SGTM and GGM gross thrust in percent of GGM gross thrust is shown in figure 12 for the 66 flight evaluation points. Also shown is the expected uncertainty from figure 11. Most of the data agree within ±3 percent and fall within the expected uncertainty band. It is not possible to separate SGTM errors from GGM errors, but the agreement with the expected uncertainty band and the lack of any strong bias in the data indicate that the SGTM and GGM accuracies were comparable.
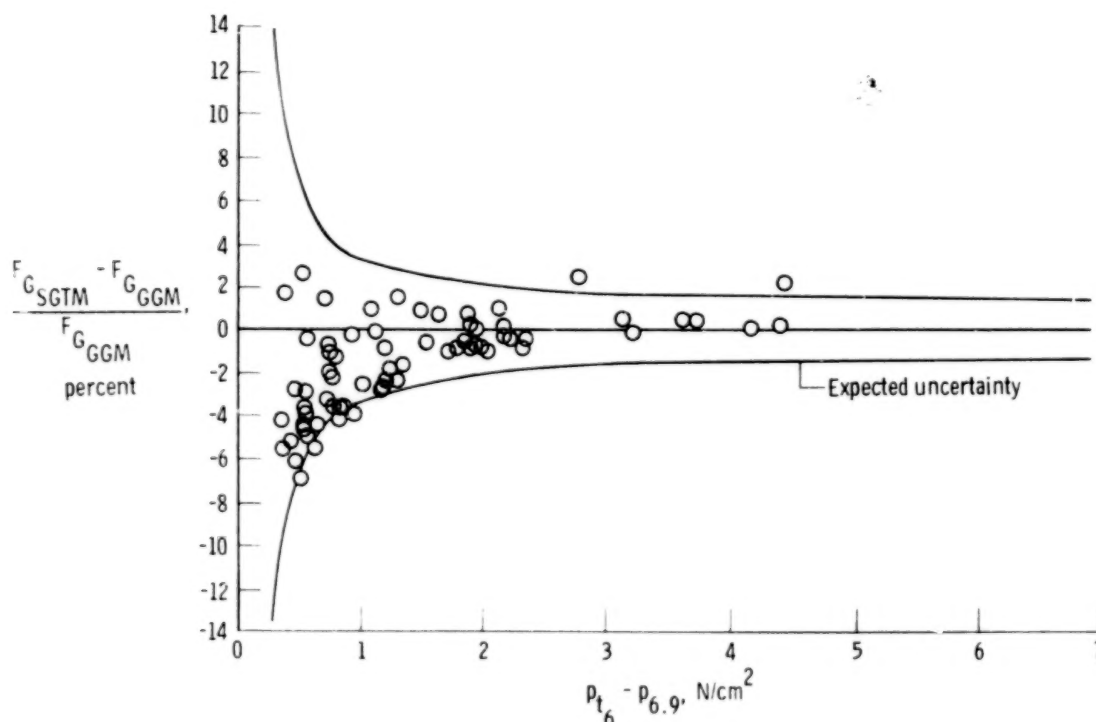

Figure 12. Difference in gross thrust between the SGTM and the GGM.

Use of Bill of Material Probe for Total Pressure at Station 6

The use of the BOM p_{t_6} probe in place of the 30 probe p_{t_6} rake was investigated for the SGTM. This probe was not used in the development of the SGTM coefficients. (For this evaluation, the GGM gross thrust was based on the 30 probe p_{t_6} measurement.) The results are shown in figure 13. Considerably more scatter is evident in the data, with errors of up to 12 percent, although most of the data fall within ±6 percent. This increase in error is due to the inadequate sampling of the BOM probe and
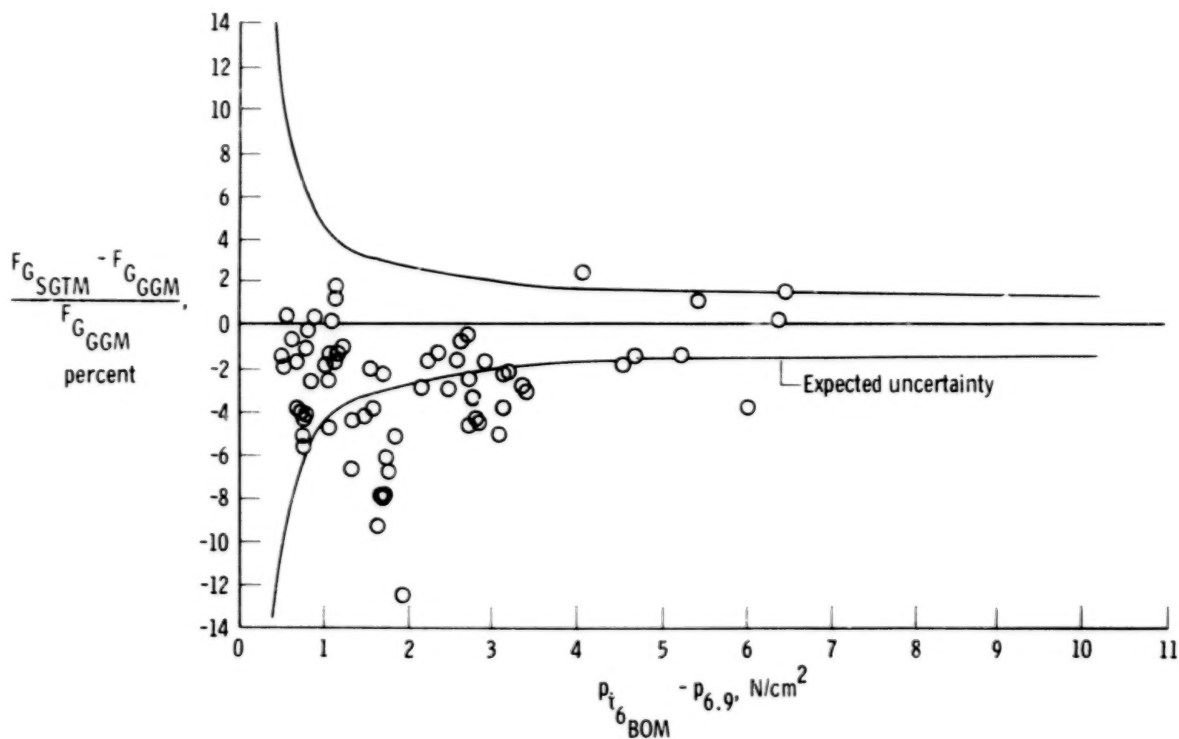
16

Figure 13. Difference between SGTM using $p_{t_{6_{BOM}}}$ and GGM gross thrust.

also to the sensitivity of the SGTM to the p_{t_6} measurement. When the BOM p_{t_6} probe was used with the GGM, the maximum errors were approximately 2 percent, a result of the fact that the GGM was less sensitive to the p_{t_6} measurement.

CONCLUDING REMARKS

A simplified gross thrust model was used to calculate the in-flight gross thrust of an F100 engine in an F-15 airplane. Gross thrust was also calculated with the gas generator method for comparison.

It was found that the two methods of gross thrust calculation agreed within ±3 percent. Most of the data fell within an estimated uncertainty band based on the measurement uncertainties and sensitivities of the two methods.

The use of a single mass averaged measurement of turbine discharge pressure in place of a 30 probe rake was found to reduce the accuracy of the simplified gross thrust model to ±6 percent.

Dryden Flight Research Center
  National Aeronautics and Space Administration
    Edwards, Calif., September 10, 1980

17

REFERENCES

1. Burcham, Frank W., Jr.: An Investigation of Two Variations of the Gas Generator Method To Calculate the Thrust of the Afterburning Turbofan Engines Installed in an F-111A Airplane. NASA TN D-6297, 1971.

2. Arnaiz, Henry H.; and Schweikhard, William G.: Validation of the Gas Generator Method of Calculating Jet-Engine Thrust and Evaluation of XB-70-1 Airplane Engine Performance at Ground Static Conditions. NASA TN D-7028, 1970.

3. Kurtenbach, Frank J.: Comparison of Calculated and Altitude-Facility-Measured Thrust and Airflow of Two Prototype F100 Turbofan Engines. NASA TP-1373, 1978.

4. McDonald, G. B.: Theory and Design of an Airborne Thrust Computing System. H036/119/FR/IV, Computing Devices (Ottawa), Aug. 1974.

5. Mackintosh, G. B.; and Dawson, J. E.: A New Technique To Compute Installed Jet Engine Thrust: Applications to Trimming for Economic and Operational Benefits. Fourth Internat. Symposium on Air Breathing Engines, Am. Inst. Aeronaut. Astronaut., P791, 1979, pp. 79-88.

6. Hamer, M. J.; and Alexander, R. I.: In-Flight Thrust Computing System Development for the Dymotech F-4C/J79-GE-15 Aircraft. AFFTC-TR-79-33, Air Force Flight Test Center, Edwards AFB, 1979.

7. Kurtenbach, Frank J.: Evaluation of a Simplified Gross Thrust Calculation Technique Using Two Prototype F100 Turbofan Engines in an Altitude Facility. NASA TP-1482, 1979.

8. Biesiadny, Thomas J.; Lee, Douglas; and Rodriguez, Jose R.: Airflow and Thrust Calibration of an F100 Engine, S/N P680059, at Selected Flight Conditions. NASA TP-1069, 1978.

9. Biesiadny, Thomas J.; Lee, Douglas; and Rodriguez, Jose R.: Altitude Calibration of an F100, S/N P680063, Turbofan Engine. NASA TP-1228, 1978.

10. F100 (3) In-Flight Thrust Calculation Deck CCD 1088-2.0, Pratt & Whitney Aircraft, 1975.

11. Shapiro, Ascher H.: The Dynamics and Thermodynamics of Compressible Fluid Flow. Vol. 1, Ronald Press Co., c.1952.

1. Report No. NASA TP-1782	2. Government Accession No.	3. Recipient's Catalog No.
4. Title and Subtitle Flight Evaluation of a Simplified Gross Thrust Calculation Technique Using an F100 Turbofan Engine in an F-15 Airplane		5. Report Date January 1981
		6. Performing Organization Code RTOP 505-11-24
7. Author(s) Frank J. Kurtenbach and Frank W. Burcham, Jr.		8. Performing Organization Report No. H-1118
9. Performing Organization Name and Address NASA Dryden Flight Research Center P. O. Box 273 Edwards, California 93523		10. Work Unit No. 506-51-34
		11. Contract or Grant No.
12. Sponsoring Agency Name and Address National Aeronautics and Space Administration Washington, D. C. 20546		13. Type of Report and Period Covered Technical Paper
		14. Sponsoring Agency Code

15. Supplementary Notes

16. Abstract

A simplified gross thrust calculation technique has been evaluated in flight tests on an F-15 aircraft using prototype F100-PW-100 engines. The technique relies on afterburner duct pressure measurements and empirical corrections to an ideal one-dimensional analysis to determine thrust. This report presents an in-flight comparison of gross thrust calculated by the simplified method to gross thrust calculated by the engine manufacturer's gas generator model. The evaluation was conducted at Mach numbers from 0.6 to 1.5 and at altitudes from 6000 meters to 13,700 meters.

The flight evaluation showed that the simplified gross thrust method and the gas generator method agreed within ±3 percent. The discrepancies between the data generally fell within an uncertainty band derived from instrumentation errors and recording system resolution.

17. Key Words (Suggested by Author(s)) In-flight thrust calculation Jet engines	18. Distribution Statement Unclassified-Unlimited STAR category 07
19. Security Classif. (of this report) Unclassified	20. Security Classif. (of this page) Unclassified	21. No. of Pages 22	22. Price* A02

19

END

February 27/981